University of Trieste

Department of Engineering and Architecture

Corso di

Termofluidodinamica Computazionale

Evaluation of the flow in an asymmetric plane diffuser with different turbulence models

Supervisor:

prof. Enrico Nobile

Students:

Francesco De Fazio

Marco Ferrari

Academic Year 2017/2018

Abstract

Numerical simulations of the turbulent flow in an asymmetric two-dimensional diffuser are performed using three turbulence models: $k-\varepsilon$, *SST* and *SSG RSM*.

A comparison with experimental data was carried out on the velocity, the turbulent kinetic energy and C_p profiles, and the separation and reattachment points. A set of simulations was performed in order to make the discretization and the convergence errors negligible, and therefore to estimate the modelization errors. Results showed that the *SSG* model provides a good agreement with experimental measurements; *SST* model does contemplate the recirculation zone but slightly mispredicts the values for velocity, turbulent kinetic energy, C_p, and separation and reattachment points position. The $k-\varepsilon$ model shows a poor agreement with experimental data because it does not predict any recirculating flows.

All the simulations were performed using ANSYS CFX 19.0, while the meshes were created with ICEM CFD 19.0. The ANSYS software suite was used under the *Academic* license, which set a superior limit to the number of nodes (512K).

Contents

1 Introduction

In this project we investigated the turbulent flow in an asymmetric plane diffuser; this experiment received a lot of attention in the 90s because it has fully developed turbulent inlet conditions, and it includes separation from a smooth wall, subsequent reattachment, and redevelopment of the downstream boundary layer[2]. These features represented a benchmark for turbulence models.

The goal of this work is therefore to compare the results of some models of turbulence with the experimental data. The turbulence models that we used are:

- standard $k - \varepsilon$;
- Shear Stress Transport (SST);
- SSG Reynolds stress model ($SSG\ RSM$).

2 Experimental tests

The asymmetric plane diffuser is made of three sections: inlet, diffuser and outlet (Figure 1). Both inlet and outlet are rectangular ducts with an height of H and $4.7H$, respectively. The diffuser, which is $21H$ long, connects the inlet to the outlet and is characterized by a wall inclined at almost 10°, while the other side is straight.

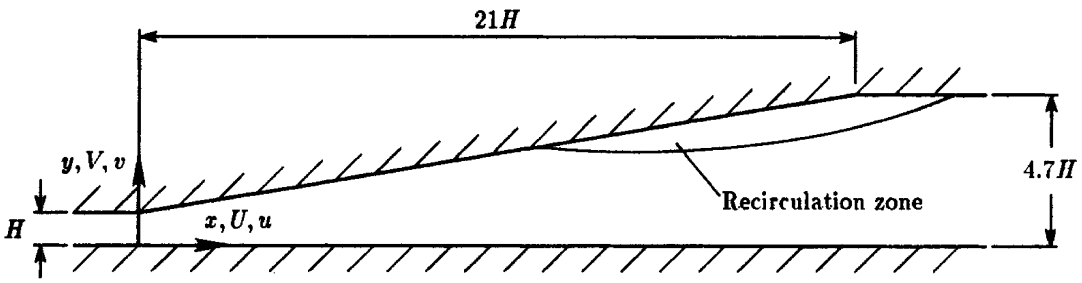

Figure 1: Geometry of the asymmetric plane diffuser[1].

The experiments were performed by *Obi et al.* in an open air flow system; the inlet boundary condition was the fully developed two-dimensional turbulent channel flow at $Re = 2.0 \times 10^4$. The two-dimensionality of the flow was examined and confirmed by the authors [1]. In the experimental setup, the outlet channel was extended about $40H$ downstream; it was observed that flow separation occurred only on the inclined wall of the diffuser.

3 Problem setup

The problem under investigation is a steady-state turbulent flow in a 2D geometry. The circulating fluid is air at room temperature.

3.1 Definition of the problem

From the references, all dimensions were non-dimensionalized in terms of H. So, in order to proceed with the definition of the problem, we chose $H = 0.1\ m$. This leads also to an inlet bulk velocity

$$U_\infty = \frac{Re \cdot \mu}{H \cdot \rho} = 3.09\ m/s$$

with the assumptions of $\mu = 1.831 \cdot 10^{-5}\ N \cdot s/m^2$ and $\rho = 1.185\ kg/m^3$.

3.2 Preliminary investigations

In order to obtain a fully developed turbulent flow at the beginning of the diffuser, an adequate length of the inlet duct must be set. To the best of our knowledge, no specific formulas for a rectangular duct are present in literature. Therefore, we performed a simulation on a simple rectangular duct of height H and length L to evaluate the minimum length to obtain a flow which can be considered as fully developed. This quantity can be however estimated by considering the entrance length of a pipe and introducing the hydraulic diameter $D_h = \frac{4A}{P}$; then the entrance length is computed as

$$\overline{L} = 4.4 \cdot D_h \cdot (Re)^{1/6} = 4.68\ m$$

Obviously the problem was set with the parameters of our main problem, because we expect that the length will depend on the Reynolds number. Thus, we chose $H = 0.1\ m$ and $L = 6.0\ m$.

Performing the simulation with residuals of 10^{-5} and a medium refined mesh[1] gave the results shown in Figure 2. In this figure, the quantity *error* is defined as follows:

$$err_j = \sum_i (v_i^{(ref)} - v_i^{(j)})^2$$

where $v^{(ref)}$ is the velocity at the outlet of the duct and $v^{(j)}$ is the velocity at the j-th reference location along x-axis.

As shown in Figure 2 the flow is fully developed after 5.0 m, because the variation of the profile can be neglected; this value is in agreement with the theoretical value calculated before.

We performed also a simulation using the fully developed turbulent velocity profile as an inlet boundary condition and we observed that the profile did not change, as expected. Thus we can assert that the velocity profile obtained through this simulation is a good approximation of the velocity profile of a fully developed turbulent flow.

[1] The mesh used had 50000 nodes and 24451 elements.

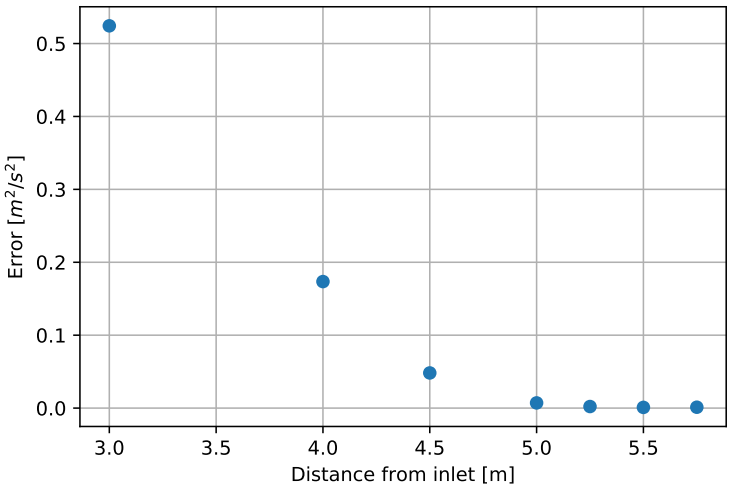

Figure 2: Evaluation of entrance length for a turbulent flow with $Re = 2.0 \cdot 10^4$ in a straight rectangular duct with $H = 0.1\ m$. Target residuals for convergence 10^{-5}.

3.3 Domain definition

Three domains were used to investigate the effect of the length after the diffuser; each domain is characterized by a different downstream length, indicated with $L3$ in Figure 3. The values of $L3$ are reported in Table 1.

Domain	H1	H2	L1	L2	L3
Small	1	4.7	5	21	44
Medium	1	4.7	5	21	59
Long	1	4.7	5	21	79

Table 1: Geometrical dimensions (non-dimensionalized in terms of H) for the three domains examined.

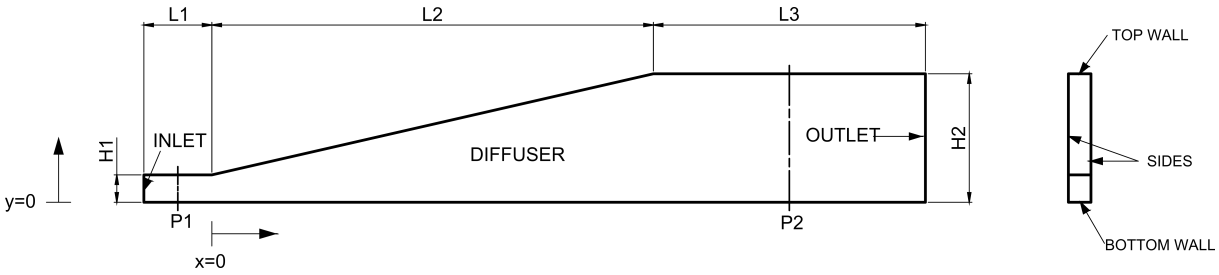

Figure 3: Computational domain.

3.4 Boundary conditions

A set of boundary conditions must be set in order to perform the simulations.

- **Inlet**: the turbulent fully developed profile obtained from the preliminary investigation was used as an inlet boundary condition for the diffuser. By doing this, we reduced the length of the inlet rectangular duct, in order to save some computational time. In the turbulence setting in CFX, a condition of *zero-gradient* was chosen; in fact, after some runs of the simulations, this condition seems to achieve better agreement with experimental results. Moreover, in the CFX reference guide, this option is suggested for fully developed turbulent flows.

- **Outlet**: a standard outlet BC was assigned to the outlet. A relative pressure of 0 Pa was set.

- **Wall**: for both top and bottom wall the boundary condition was no-slip wall, with the option of smooth wall.

- **Symmetry**: in order to perform a 2D simulation in CFX, a symmetry condition must be set on the sides of the domain, otherwise the CFX solver returns an error.

A summary of the boundary conditions is reported in Table 2.

Part	Condition	Value
INLET	Inlet	From profile
OUTLET	Outlet	$p = 0\ Pa$
TOP_WALL, BTM_WALL	No-slip smooth wall	
SIDES	Symmetry	

Table 2: Boundary conditions.

3.5 Grid generation

In the following simulations different meshes were used. A summary of all the meshes used is reported in Table 3. In particular:

- in the convergence criterion section, the simulations were performed on a *coarse* mesh and *small* domain (A1);

- in the domain influence section, the simulations were performed on the three domains, all of them with a *coarse* mesh. In this case the number of nodes of the meshes slightly differs because of the different downstream lengths (A1, B1, C1);

- in the mesh independence section, successive mesh refinements were done on the *medium* domain (B1, B2, B3), focusing on the expected zone of recirculation.

Domain	Mesh		
	Coarse	Medium	Fine
Small	A1	-	-
Medium	B1	B2	B3
Large	C1	-	-

Mesh	Element	Nodes
A1	6438	13380
B1	7598	15780
B2	26963	54960
B3	62923	127440
C1	9193	19080

Table 3: Meshes denominations (left) and dimensions (right).

All the meshes used were designed with the goal of keeping the y^+ value constant: by doing this the wall functions used were the same for all the meshes. In particular we set the height of the first node in order to obtain $y^+ \simeq 1$ and strictly $y^+ < 3$. In this way the first cell center is placed in the viscous sublayer.

Moreover, all the meshes were extruded by only one element, in order to be compatible with the CFX solver.

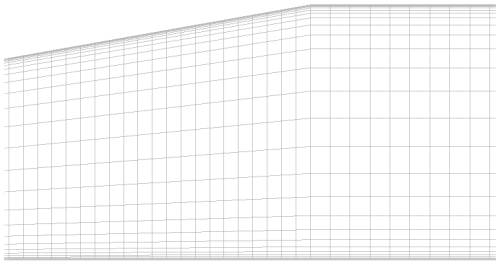

Figure 4: Close view of the coarse mesh.

As quality indexes, we checked the determinant $3 \times 3 \times 3$ and the angle: all the meshes were characterized by a determinant greater then 0.955 and an angle greater than 80°.

4 Simulations

All the following evaluations were performed with the *SST* model for turbulence. For all the simulations the *High Resolution* option was adopted for advection scheme and the *First Order* option was chosen for turbulence numerics. The options for the fluid timescale control were left as default.

Two planes *P1* and *P2* were defined at $x = -0.3\ m$ and $x = 5.0\ m$, respectively; the pressure was evaluated on these planes in order to have an index of variability of the results upon residuals, domain or grid, depending on the case addressed.

4.1 Convergence criterion

We investigated the influence of the residual on the results. The pressure was evaluated on the two planes $P1$ and $P2$ for different values of target residual in the solver.

From Table 4 it can be seen that the adoption of a value smaller than 10^{-5} for the RMS residuals results in a negligible change in the data for Δp. Hence, for the next simulations the value of 10^{-5} is chosen for residual target.

Residual RMS	**Mesh**	Δp $[Pa]$
10^{-3}	A1	3.3306
10^{-4}		3.1921
10^{-5}		3.1932
10^{-6}		3.1937

Table 4: Influence of the residual.

4.2 Domain influence

We tested the influence of the downstream length of the diffuser by changing the computational domain; the differences of pressure evaluated on the two planes are reported in Table 5.

Even if the variation of pressure between the shortest and the longest is quite negligible, we chose to perform the next simulations on the medium domain. This choice leads to an increase in the computational time, but it guarantees that the results are not biased by the downstream length.

Domain	**Mesh**	Δp $[Pa]$
Small	A1	3.1932
Medium	B1	3.1933
Long	C1	3.1933

Table 5: Influence of the downstream length.

4.3 Grid independence

Successive refinements were done on the medium domain in order to obtain a grid independent solution. The results are reported in Table 6.

Mesh		Δp $[Pa]$
Coarse	B1	3.1933
Medium	B2	3.1509
Fine	B3	3.1639

Table 6: Influence of the mesh dimension.

It can be seen that the difference between the meshes B2 and B3 is of the order of 10^{-2} Pa. Given the very high computational cost associated with the B3 mesh, we

adopted the computationally cheaper B2 mesh for the following simulations and assumed this value as an accettable uncertainty on our data. To confirm our grid independence test, in Figure 5 we compare C_p for the three meshes used. It can be seen that there is almost no difference between the medium and fine mesh, while the coarse mesh slightly overestimates C_p.

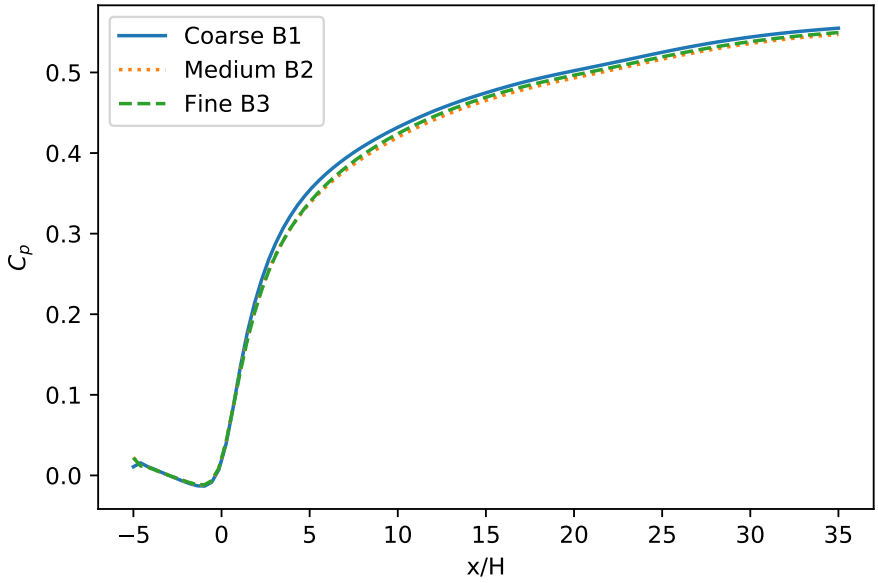

Figure 5: Comparison of C_p among the meshes.

5 Results and discussion

In this section, we are going to compare the experimental data with the results produced by the simulations with the $k-\varepsilon$, $k-\omega$ *SST* and *SSG RSM* turbulence models.

Once we defined a grid independent solution, we studied the behaviour of the turbulence models. We were able to use the models on the same mesh because of the scalable wall functions[2] implemented in CFX on the $k-\varepsilon$ and *SSG* models.

From [1] the velocity and the turbulent kinetic energy profiles are available at three location in the diffuser section ($x/H = 7.2, 13.2, 19.2$). The C_p curve is also available:

$$C_p = \frac{p - p_0}{\frac{1}{2}\rho U_\infty^2}$$

where p is the pressure measured on the straight wall of the diffuser and p_0 is the pressure measured at $x/H = -3$.

In Figure 6 we reported the plots of C_p for both experimental and numerical data.

[2]The scalable wall functions enable solutions on arbitrarily fine near-wall grids.

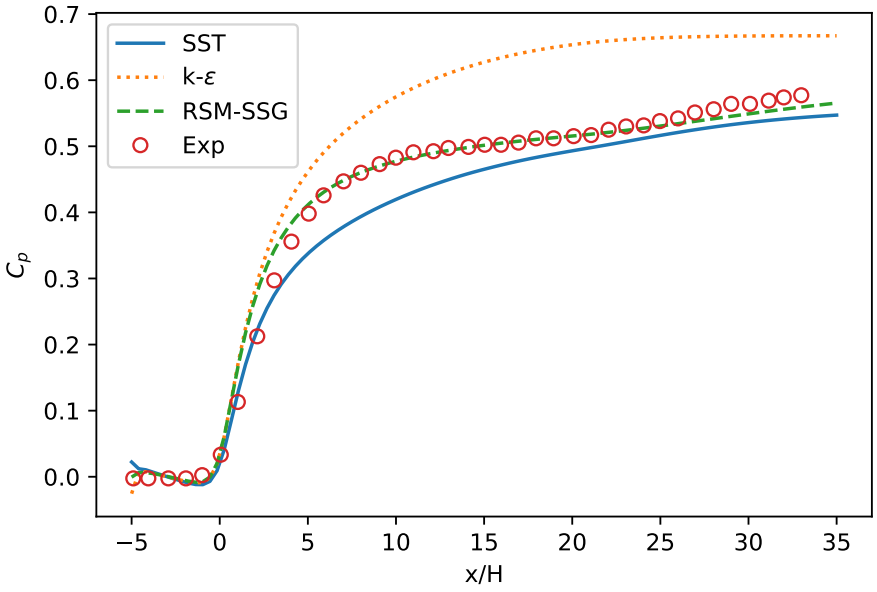

Figure 6: Comparison of C_p for different models of turbulence and experimental values.

The model that better estimates the curve of C_p is the *SSG RSM*, while the worst is the $k-\varepsilon$. These results are reasonable: in fact, the *SSG* model does not use the eddy viscosity hypothesis, but it solves the equations for the transport of Reynolds stresses in the fluid. So the *SSG* is capable to describe problems where the anisotropy of the Reynolds stress tensor is crucial, like the case studied[1].

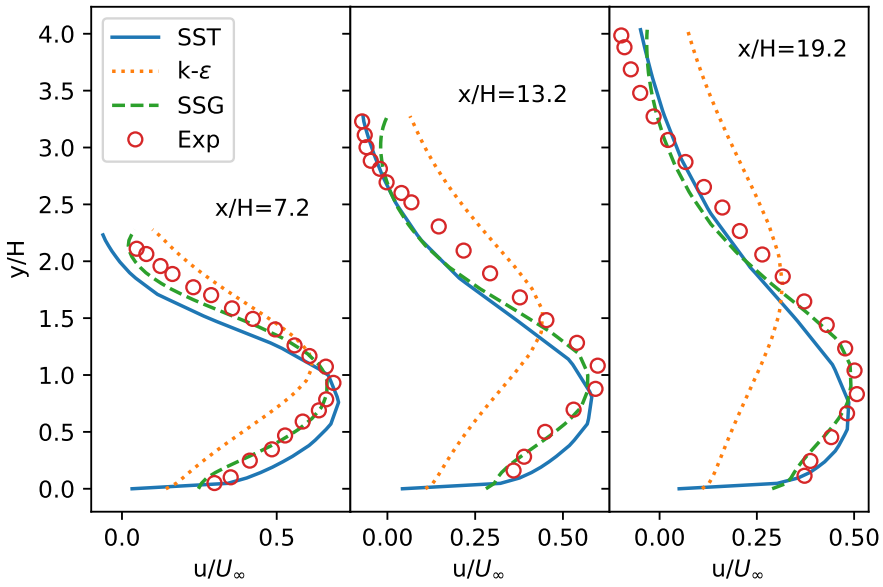

Figure 7: Velocity comparison at different x/H.

The predictions of *SST* are not so far from the experimental values; bearing in mind that this is a two-equation model like $k-\varepsilon$, our results indicate that in this case the

SST is capable of better prediction than the $k-\varepsilon$. This conclusion is true even for the velocity profile. In fact, as shown in Figure 7, the $k-\varepsilon$ model does not provide any recirculation zone, while *SST* does (negative values of u near the diffuser top wall). The profile is similar to the experimental one, but the maximum values and positions are slightly mispredicted. On the other hand, *SSG RSM* does provide very good results in accordance to the experimental measurements.

The described situation does not vary considering the turbulent kinetic energy profiles. The *SSG RSM* is once again the model which provides better results in comparison with the experimental data. In this case, as it can be seen in Figure 8, the predictions are slightly erroneous even for *SSG*.

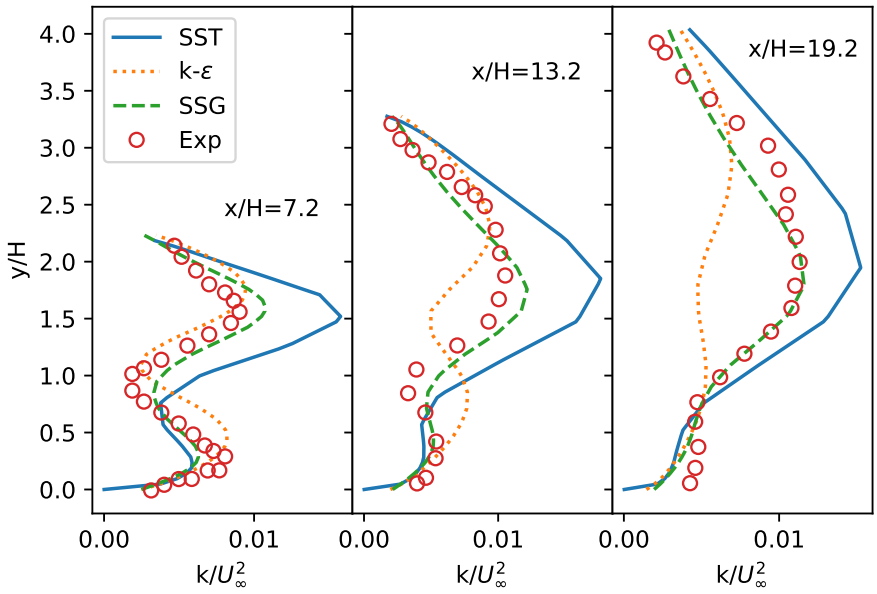

Figure 8: Turbulent kinetic energy comparison at different x/H.

	Turbulence model			Experimental
	SST	$k-\varepsilon$	*SSG RSM*	
Separation	0.3	-	1.3	1.1
Reattachment	2.9	-	2.4	2.6

Table 7: Position of separation and reattachment points in meters.

A key point in the performance evaluation of the models is the prediction of the separation and reattachment points. In a separation or reattachment point the mean velocity parallel to the wall is zero; in CFD-Post we looked for these points by plotting the mean velocity as a function of x-coordinate along a line positioned at the top wall. As reported in Table 7, the *SSG* model confirms its good predictive capability, while the *SST* overestimates both separation and reattachment points. The $k-\varepsilon$ model did not provide

any points because it does not perform well for boundary layers with an adverse pressure gradient[3].

6 Conclusions

In this work we studied the turbulent flow in an asymmetric plane diffuser. The experimental values were available in literature, so we could compare them with the results from three different turbulence models: $k-\varepsilon$, *SST* and *SSG RSM*.

From our analysis, *SSG* showed better prediction capabilities over the others. This is in accordance with what we expected: both $k-\varepsilon$ and *SST* are two-equation turbulence models, while *RSM* models are characterized by the use of additional transport equations. The accuracy provided by *SSG* is then justified, but it is obtained at a higher computational cost as you can see in Table 8.

Comparing *SST* with $k-\varepsilon$, once again we obtained results that confirmed our expectations: the $k-\varepsilon$ model did not predict any recirculating flows, which were present in this case. *SST* is a low-Reynolds model and can therefore predict with greater accuracy the flow separation if the mesh is close enough to the wall.

	Turbulence model		
	SST	$k-\varepsilon$	*SSG RSM*
CPU time	2.02	1	2.49
Iterations	1.90	1	1.85
CPU time per iteration	1.06	1	1.35

Table 8: Computational cost for the turbulence models used. All the values are normalized in relation to the $k-\varepsilon$ model.

References

[1] Obi, S., Aoki, K. and Masuda, S. "Experimental and computational study of turbulent separating flow in an asymmetric plane diffuser". *Ninth Symposium on Turbulent Shear Flows*, Kyoto, Japan. August 16-19, 1993. p 305.

[2] Buice, Carl U., and John K. Eaton. "Experimental Investigation of Flow Through an Asymmetric Plane Diffuser." *Journal of Fluids Engineering*, vol. 122, no. 2, 2000, p. 433., doi:10.1115/1.483278.

[3] Wilcox, D.. "Turbulence modeling for CFD". 3rd ed. *DCW Industries*, 2006, p.181.